

# Development of rhomboidal acoustic lens constructed with phononic crystal

フォノンニック結晶構造を用いた菱形音響レンズの開発

Takenobu Tsuchiya<sup>1†</sup>, Tetsuo Anada<sup>1</sup>, Nobuyuki Endoh<sup>1</sup>, Sayuri Matsumoto<sup>2</sup>, Kazuyoshi Mori<sup>3</sup>

(<sup>1</sup>Faculty of Engineering, Kanagawa Univ.; <sup>2</sup>The Port and Airport Research Institute;

<sup>3</sup>Department of Earth and Ocean Sciences, National Defense Academy of Japan)

土屋 健伸<sup>1†</sup> 穴田 哲夫<sup>1</sup> 遠藤 信行<sup>1</sup> 松本 さゆり<sup>2</sup> 森 和義<sup>3</sup>

(<sup>1</sup>神奈川大学 工学部 <sup>2</sup>(独) 港湾空港技術研究所 <sup>3</sup>防衛大学校 地球海洋)

## 1. Introduction

The imaging system with acoustic lens have been to develop in the underwater field [1-2]. Authers reported the characteristics of planate acoustic lens constructed with phononic crystal structures (PhC)[3]. Planate acoustic lens with negative refractive index was possible to focussing a sound when spherical wave was insident to the plate. However, planate acoustic lens has lower gain against aspherical lens. For the formulation of a rhomboidal high gain lens [4], we design the rhomboidal acoustic lens by focussing the plain wave. In previous study, we measured the characteristics of negative refractive index depended on incidence angle at the plate of PhC for the design rhomboidal lens fabricated by PhC [5].

In this paper, we design a rhomboidal acoustic lens, as shown in Fig. 1. We reported the basic property of the rhomboidal acoustic lens for the development of imaging system with acoustic technology in ocean.

## 2. Configuration of Rhomboidal Acoustic Lens Constructed with PhC

Figure 1 shows the configuration of rhomboidal acoustic lens constructed with PhC. PhC composed of rhomboidal acoustic lens configured at triangular lattices. The PhC was made by stainless steel rods, at which diameter and thickness are defines  $a=0.7$  mm and  $d=1.5$  mm, as shown in Fig. 1. Layer's number of this PhC to the propagation direction  $z$  is thirteen. Around medium of rods assume the pure water. Sound velocity and density of water and stainless steel rods was shown in Table I. Cut angle of Front and back plain at rhomboidal acoustic lens is  $\theta = 30^\circ$ , respectively. Negative refractive index in case of  $\theta = 30^\circ$  is -0.56 from prrevious study [5]. We simulated the focussinng propaties of rhomboidal acoustic lens caululated by elastic finite difference time domain method [5].

-----  
kenshin@kanagawa-u.ac.jp

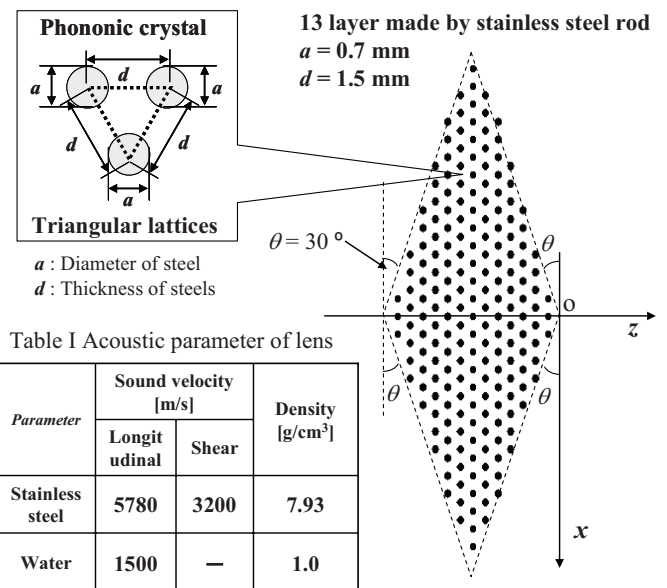


Fig. 1 Configuration of rhomboidal acoustic lens constructed with PhC.

## 3. Simulation and Results

### 3.1 Frequency Characteristic

To obtain the basic frequency characteristics of rhomboidal acoustic lens, we simulated sound pressure distribution in  $z$ - $x$  plain. Figure 2 (a), (b), and (c) show calculation results of sound pressure at frequency  $f = 500, 700,$  and  $900$  kHz. Focusing effect by rhomboidal acoustic lens appeared the sound field backward of lens at  $f = 700, 900$  kHz. On the other hands, focal spot do not appeared the sound field backward of lens at  $f = 500$  kHz. Figure 3 (a) and (b) show the sound pressure distribution in propagation direction  $z$  and transverse direction  $x$ . Focal range from edge at second plane of lens are  $7.0$  mm and  $34.0$  mm at  $f = 700, 900$  kHz, respectively.  $-3$  dB beam widths about normalized sound pressure distribution at transverse direction  $x$  are  $0.54$  mm and  $8.2$  mm at  $f = 700, 900$  kHz. It has very narrow beam focusing by rhomboidal acoustic lens at  $f = 700$  kHz.

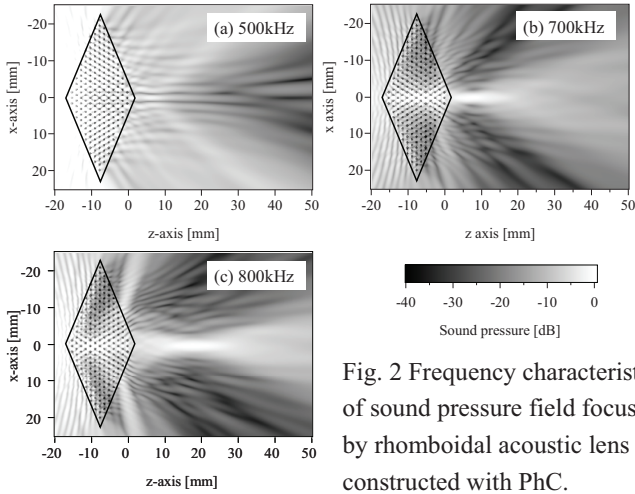


Fig. 2 Frequency characteristics of sound pressure field focusing by rhomboidal acoustic lens constructed with PhC.

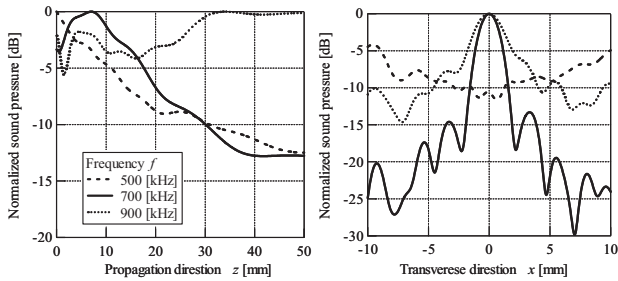


Fig. 3 Sound pressure distribution on axis when frequency  $f$  is changed from 500 kHz to 900 kHz. (a) is propagation direction  $z$ , (b) is transverse direction  $x$  at focal point.

### 3.2 Effect of thickness of rods

To improve the performance of rhomboidal acoustic lens, we simulated the focusing properties of lens depended on thickness of rod at PhC. Figure 4 shows calculation results of sound pressure at thickness of rod  $d = 0.5, 0.7$ , and  $1.3$  mm. As shown in all Figure4's, focal spot appeared the sound field backward of lens. However, as shown in Fig. 5 (a), gain at focal point in case at  $d = 0.5$  mm is lower than other cases. In addition, large side-robe exists in sound pressure distribution at focal point. Figure 5 (b) shows the sound pressure distribution in transverse direction  $x$ .  $-3$  dB beam widths about at focal point are  $0.54$  mm in three cases. But, in cases at  $d = 0.5$  mm, and  $1.3$  mm, high level side-robe are appeared. However, in cases at  $d = 0.7$  mm, side-robe level is lower about  $-15$  dB. As a result, we designed a rhomboidal acoustic lens and obtained the basic properties of rhomboidal acoustic lens.

### 4. Conclusions

In this paper, we designed the rhomboidal acoustic lens constructed with PhC. In future work, we will optimize the performance of rhomboidal

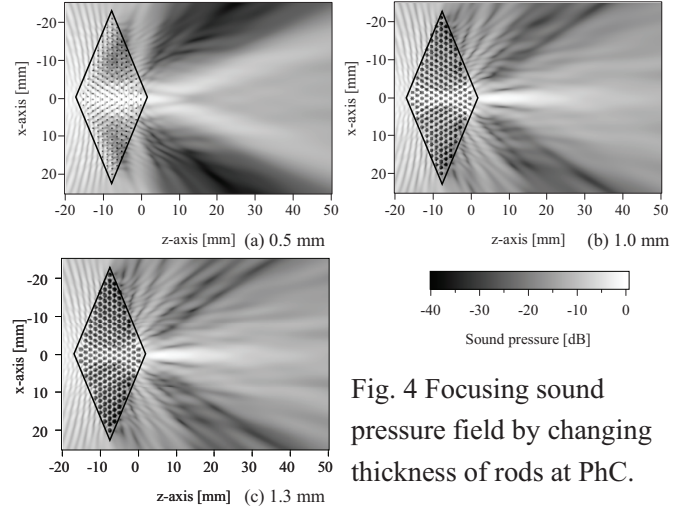


Fig. 4 Focusing sound pressure field by changing thickness of rods at PhC.

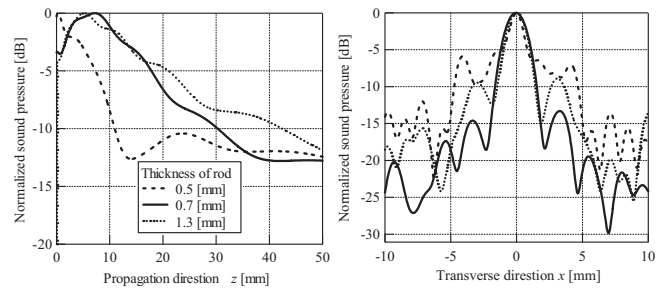


Fig. 5 Sound pressure distribution on axis when thickness of rod  $d$  is changed from  $0.5$  mm to  $1.3$  mm. (a) is propagation direction  $z$ , (b) is transverse direction  $x$  at focal point

lens using for design of asymmetrical rhomboidal lens. Furthermore, we designed the rhomboidal acoustic lens using by genetic algorithm to short the calculation time for the optimization of asymmetrical rhomboidal lens.

### Acknowledgment

This study was partly supported by a Grant-in-Aid for Scientific Research (C) (No. 2456092) from the Ministry of Education, Culture, Sports, Science and Technology, Japan. In addition, this work was partly supported by the Research and Development Committee Grants of the Japan Society of Ultrasonics in Medicine at 2011 to 2012.

### References

1. K. Mori, *et. al.* : Jpn. J. Appl. Phys. **51** (2012) 07GG10
2. K. Mori, *et. al.* : Jpn. J. Appl. Phys. **52** (2013) 07HG02.
3. T. Tsuchiya, *et. al.* : Jpn. J. Appl. Phys. **51** (2012) 07GG11.
4. S. Zhang, L. Yin, and N. Fang: Phys. Rev. Lett. **102** (2009) 194301.
5. T. Tsuchiya, *et. al.* : Proccof USE **33** (2012) 121 .